AD-A106 222 MARTIN MARIETTA LABS BALTIMORE MD F/G 11/1
MECHANICAL PROPERTIES OF ADHESIVELY BONDED ALUMINUM STRUCTURES --ETC(U)
OCT 81 J S AHEARN, G D DAVIS, A DESAI N00014-80-C-0718
UNCLASSIFIED MML-TR 81-46C NL

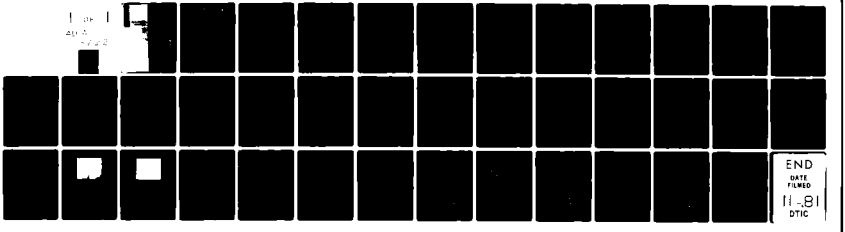

END
DATE FILMED
11-81
DTIC

MARTIN MARIETTA

Martin Marietta Laboratories

MML TR 81-46c

MECHANICAL PROPERTIES OF ADHESIVELY BONDED ALUMINUM STRUCTURES PROTECTED WITH HYDRATION INHIBITORS

End-of-First-Year Report

October 1, 1981

Unclassified

Prepared for

Department of the Navy
Office of Naval Research
Arlington, Virginia 22217

Prepared by

Martin Marietta Laboratories
1450 South Rolling Road
Baltimore, Maryland 21227-3898

Under

ONR Contract N00014-80-C-0718

Unclassified

SECURITY CLASSIFICATION OF THIS PAGE (When Data Entered)

REPORT DOCUMENTATION PAGE	READ INSTRUCTIONS BEFORE COMPLETING FORM
1. REPORT NUMBER	2. GOVT ACCESSION NO. AD-A106 222 / 3. RECIPIENT'S CATALOG NUMBER
4. TITLE (and Subtitle) MECHANICAL PROPERTIES OF ADHESIVELY BONDED ALUMINUM STRUCTURES PROTECTED WITH HYDRATED INHIBITORS	5. TYPE OF REPORT & PERIOD COVERED End-of-First-Year Report 7-1-80 to 6-30-81
	6. PERFORMING ORG. REPORT NUMBER MML-TR 81-46c
7. AUTHOR(s) J.S. Ahearn, G.D. Davis, A. Desai, J.D. Venables	8. CONTRACT OR GRANT NUMBER(s) N00014-80-C-0718
9. PERFORMING ORGANIZATION NAME AND ADDRESS Martin Marietta Laboratories 1450 South Rolling Road Baltimore, Maryland 21227-3898	10. PROGRAM ELEMENT, PROJECT, TASK AREA & WORK UNIT NUMBERS
11. CONTROLLING OFFICE NAME AND ADDRESS Department of the Navy Office of Naval Research Arlington, Virginia 22217	12. REPORT DATE October 1, 1981
	13. NUMBER OF PAGES 38
14. MONITORING AGENCY NAME & ADDRESS(if different from Controlling Office) Baltimore DCAS Management Area 300 East Joppa Road, Room 200 Towson, Maryland 21204	15. SECURITY CLASS. (of this report) Unclassified
	15a. DECLASSIFICATION/DOWNGRADING SCHEDULE

16. DISTRIBUTION STATEMENT (of this Report)

Unlimited Distribution

This document has been approved for public release and sale; its distribution is unlimited.

17. DISTRIBUTION STATEMENT (of the abstract entered in Block 20, if different from Report)

18. SUPPLEMENTARY NOTES

19. KEY WORDS (Continue on reverse side if necessary and identify by block number)

adhesive bonding, corrosion inhibitors, organic inhibitors, aluminum oxide hydration, wedge tests, durability

20. ABSTRACT (Continue on reverse side if necessary and identify by block number)

(over)

DD FORM 1 JAN 73 1473

Unclassified

SECURITY CLASSIFICATION OF THIS PAGE (When Data Entered)

Our research has shown that the adsorbed monolayer inhibitor films that slow the conversion of Al-oxide to hydroxide substantially improve the bond durability of 2024Al adherends prepared with the Forest Products Laboratory process (FPL). In particular, an inhibitor coating of nitrilotris (methylene) phosphonic acid produced a bond durability in adherends prepared with the FPL process that was nearly the same as that in samples prepared with the otherwise more durable phosphoric acid anodization process (PAA). As determined by x-ray photoelectron spectroscopy, the inhibitor coverage needed to produce the maximum improvement in bond durability was approximately one monolayer. Increase in coverage above the presumed monolayer value did not produce better durability. Surface treatment with phosphoric acid rather than phosphonic acid was ineffective in producing better durability of adherends prepared with the FPL process. Analysis of the results suggests that a compound's effectiveness in improving bond durability of adherends prepared with the FPL process depends on both its ability to inhibit the conversion of Al-oxide to hydroxide and to form chemical bonds with the adhesive.

TABLE OF CONTENTS

LIST OF TABLES

LIST OF FIGURES

I. INTRODUCTION

Two important factors that determine the overall performance and success of adhesively bonded aluminum structures are the initial bond strength of the adherend/adhesive interface, and the stability of the interface in a humid environment. Recent studies at Martin Marietta Laboratories (1) have indicated that the initial bond strength of commercial aerospace bonding processes is determined principally by physical interlocking between the oxide on the Al adherend and the adhesive.

The Al-oxide morphologies of two commercial processes are illustrated in Figs. 1 and 2. The Forest Products Laboratory process (FPL) produces an oxide morphology consisting of oxide cells roughly 400 Å in diameter and whisker-like structures 400 Å high (Fig. 1). The phosphoric acid anodization process (PAA) also produces an oxide morphology consisting of oxide cells and whiskers (Fig. 2), but the cells are much higher (~3,000 Å) compared with those produced by FPL. In both cases, the rough oxide surface interlocks with the overlaying adhesive to form a much stronger bond than with a smooth oxide. Indeed, tests of the initial bond strength of adhesively bonded structures properly prepared with either the FPL or PAA processes show that the bondments always fail cohesively. In contrast, tests where the adherend morphology is smooth, and therefore where the bond strength is determined exclusively by chemical reaction of the adherend surface and the adhesive, show that bondments mostly exhibit an adhesive type of failure mode (1).

The long-term durability of the Al-oxide adhesive bond is determined to some extent by physical interlocking, but recent evidence from our

research (2) indicates that bond durability is also controlled by conversion of the original adherend oxide to a hydroxide in the presence of moisture. In discussing bond durability, a distinction must be drawn when comparing durability observed with a smooth adherend oxide morphology and the durability of a rough one. For adherends with smooth morphology, the bond strength depends on the chemical interaction between the Al-oxide surface and adhesive molecules. Water penetration to a crack tip can disrupt the chemical bonds between Al-oxide and polymer molecules. Breaking of these bonds then causes crack propagation. Chemical bonds can break relatively easily since bonding generally occurs through weak van der Waals forces.

For adherends with rough oxide morphology, the breaking of chemical bonds by water does not affect crack propagation because physical interlocking of the adhesive and oxide prevents it. Crack movement is only possible if the interlocking of adhesive and oxide is somehow destroyed. Our recent work (2), indicates that the conversion of the Al-oxide to Al-hydroxide disrupts the interlocking and degrades the bond.

Bond durability of adherends prepared by the PAA process is substantially better than that of adherends prepared with FPL (3). Also, the incubation time for converting Al-oxide to Al-hydroxide is much longer for adherends prepared by PAA than for those prepared by FPL, suggesting that the ability of the oxide to resist attack by moisture is a critical element in improved bond durability (2). However, the surface morphology of the two adherends is somewhat different (Figs. 1 and 2), so bond durability may differ because of oxide stability and the extent of oxide-adhesive interlocking.

We are currently researching the interplay of oxide morphology and stability and its effect on the durability of adhesive bonds. To separate these factors, we prepared adherends using the FPL process and then treated them in solutions containing inhibitors (phosphonic or phosphoric acid) that were expected to stabilize the oxide against conversion to hydroxide. The treatment of the adherend with hydration inhibitors increases the oxide stability, but does not alter the oxide morphology, so the oxide and adherend still interlock. Experiments were designed to isolate and study the role of oxide stability in determining bond durability. In this report, we present the correlated results of adherend surface chemistry, surface morphology, oxide stability, and bond durability to demonstrate the importance of the Al hydration reaction in bond durability.

II. EXPERIMENTAL METHOD

A. Surface Preparation of Test Coupons and Panels

2024Al was used for most of the work presented here, although several measurements were performed using 2024Al clad with a 1000 series Al alloy. Unless otherwise noted, the particular material for any given test should be understood to be 2024Al bare.

The test coupons and panels were prepared according to the flow chart in Fig. 3. The panels were degreased by immersion in an agitated solution of Turco 4215 (44 g/l)* at 65°C for 15 min, followed by rinsing in distilled deionized water. FPL treatment consisted of immersion in an agitated aqueous solution of sodium dichromate dihydrate (60 g/l) and sulfuric acid (17% v/v) held at 65°C for 15 min, followed by rinsing in distilled deionized water and air drying. The PAA process consisted of immersion of panels in a 10wt% phosphoric acid solution while applying a potential of 10V between the panels and an Al cathode for 20 min, a final rinse in distilled deionized water, and air drying.

The treatment of the panels in inhibitor solutions after the FPL process consisted of immersion in the aqueous inhibitor solution at room temperature or at 80°C for 30 min, followed by rinsing in distilled deionized water and air drying.

Several inhibitors were studied, including nitrilotris (methylene) phosphonic acid (NTMP), amino methyl phosphonic acid (AMP), hydroxy methyl

---

* An alkaline cleaning agent manufactured by Turco Products.

phosphonic acid (HMP), and phosphoric acid (PA). The structure of the deprotonated molecules are shown schematically in Fig. 4.

B. Incubation Time Measurements

We made incubation time measurements by direct visual observation and ellipsometry. For both methods, we boiled deionized distilled water for 5 min to lower the dissolved O_2 concentration and then cooled it to 80°C. For visual observations, we immersed the sample in the water directly and determined the time after immersion when gas bubbles formed on the surface and when the color of the surface changed. The change in color was a direct indication that the Al-oxide had hydrated [as determined by examination of the sample in the STEM (scanning transmission electron microscope)].

We made ellipsometry measurements using a null balance technique where the polarizer and analyzer are rotated to extinguish the light. The point of extinction represents a null point, which is specific for the thickness and optical constants of the film. Any subsequent change in the film's nature results in a change in the null point. When the Al-oxide starts to hydrate, the null point settings for the polarizer and analyzer change. Thus, if the polarizer and analyzer are left unchanged during a measurement, an increase in the light intensity, as recorded by a photomultiplier, signals the onset of hydration.

C. Wedge Test Procedure

After surface preparation, we bonded pairs of test panels (6 x 6 x 1/8 in.) together using a water-wicking adhesive (American Cyanamide FM

123-2) under a pressure of 40 psi held for 1 hr at 120°C and cooled under pressure below 65°C. Then we cut the bonded panels into 1 x 6-in. test pieces.

The wedge test was performed by inserting a wedge between the two bonded strips and by placing the sample in a humidity chamber at 98% relative humidity at 60°C. To determine the extent of crack propagation, the test pieces were periodically removed from the humidity chamber, examined under an optical microscope, and the crack tips were located and marked. After the test was complete, usually after 150 to 160 hr, we used calipers to measure the position of the markers denoting the crack extension as a function of time.

The wedge test conditions (a water-wicking adhesive, high temperature, and no corrosion-inhibiting primer) were used to accelerate the testing procedure. In all cases, once the test pieces were inserted into the humidity chamber, the crack propagated adhesively. This is an important requirement of the test since the relative effectiveness of different inhibitors can only be determined if the failure is adhesive.

III. RESULTS

A. Inhibitor Coverage of Adherend Surfaces

A typical XPS (X-ray photoelectron spectroscopy) spectrum (Fig. 5) of an NTMP-treated 2024Al surface previously etched in FPL exhibits peaks from Al, O, Cu, C, and P; N and S were also detected on some surfaces. Al and most of the O result from the Al-oxide surface film. Cu is in the alloy and is present in enhanced concentration at the Al-oxide/Al-metal interface (1). P, N, and a small part of the O signal result from adsorbed NTMP molecules. S is a surface contaminant left after etching in FPL and is probably present as sulfate (a small part of the O signal probably results from a sulfate compound). C is a surface contaminant caused by adsorbed hydrocarbons. XPS spectra for adherend surfaces treated with other inhibitors are similar.

To determine the amount of inhibitor adsorbed on a particular adherend surface, we measured the peak height of the 2p photoelectrons from P and Al and calculated the P/Al ratio using sensitivity factors determined elsewhere (4). The P/Al ratio was taken as the relative coverage of inhibitor on the Al-oxide surface. Figure 6 and Table I summarize the results of this analysis as a function of inhibitor concentration.

The coverage of the NTMP molecule saturates at a P/Al of ~ 0.15 to 0.20 as the solution concentration increases above 5 ppm. The saturation NTMP level may represent monolayer coverage of the adherend surface (see below). The coverages obtained using HMP and AMP (~ 0.05) are substantially

below the saturation NTMP level. This difference may be related to the mechanism of adsorption and is discussed briefly below.

In the case of dilute phosphoric acid solutions, the saturation coverge (~ 0.10) is intermediate between that obtained with NTMP and HMP or AMP. The coverage of the PA-treated FPL adherends is the same as that found on adherends prepared for bonding by PAA (4).

B. Incubation Time Measurements

The incubation time for conversion of oxide to hydroxide in FPL-etched coupons was approximately 2 min when no inhibitor was used. Some coupons hydrated in as short a time as 1 min, and others, in 2.5 min. Treatment of the FPL surface with any of the inhibitors increased the incubation time considerably. For most of our work on incubation time we used NTMP, in which case some coupons with saturation coverage hydrated in 15 min while others did not hydrate at all after 23 hr of immersion in water held at 80°C.

As is evident from these numbers, the incubation time measurements on coupons treated with inhibitors had considerable scatter. It is therefore somewhat difficult to use the incubation time for quantitative comparison with wedge-test results. The experimental scatter may be caused by inclusions in the 2024Al samples, which act as nucleation sites for hydration. Once the hydration reaction nucleates at one of the inclusions, it spreads over the entire surface of the sample. We presume that the sites of the inclusions are particularly difficult to passivate because of possible, local, electrochemical reaction and because the

Al-oxide film is discontinuous there. Moisture can more easily penetrate to the Al-oxide surface, or to the Al-metal/oxide interface nucleating the hydration reaction.

Measurements also indicated that the incubation times for AMP-, HMP-, and PA-treated coupons were longer than for untreated coupons. However, only a limited number of tests were run with these inhibitors, and the incubation times again showed considerable scatter, so that typical values are difficult to determine.

We made several measurements of incubation time to compare directly the effectiveness of NTMP and AMP treatments, and NTMP and PA treatments, performing these tests at the same time on test coupons that had been prepared together. The data from these comparison tests (Table II) indicate that NTMP inhibited the hydration reaction more effectively than the other inhibitors tested. Also included in Table II are "typical" incubation times for untreated FPL surfaces and surfaces treated in NTMP solutions. Considerably more work is needed, however, to make a reliable quantitative comparison of the inhibitor effectiveness.

C. Wedge Tests

Typical wedge test results (Fig. 7) for FPL, PAA, and FPL treated with a 10-ppm NTMP solution demonstrate that the treatment of 2024Al with 10-ppm NTMP significantly improves the durability of FPL-etched adherends. Indeed, the performance of the NTMP-treated FPL adherend is nearly equivalent to that of untreated PAA adherends.

Further wedge tests on adherends treated in different-concentration NTMP solutions indicated improved performance with increasing NTMP concentration (Fig. 8). In this case, the adherend treated in the 100-ppm and 10-ppm NTMP solutions exhibited crack extensions after ~ 100 hr exposure, about the same as shown in Fig. 7 for the adherend treated by FPL and 10-ppm NTMP. The crack extension of the untreated adherend in Fig. 8 was larger than that of the untreated adherend in Fig. 7. The small difference in performance of the untreated adherends may result from differences in properties of the adhesive, small amounts of contamination from the FPL solution, or slight differences in FPL oxide morphology. The relatively large difference in performance of the adherends treated in the 10-ppm NTMP solution may be related to differences in NTMP coverage on these particular panels because results of NTMP surface coverage (presented above) indicated that coverage is very sensitive to solution concentration in the 1- to 10-ppm range. Lower adherend surface coverage should result in larger crack extensions. Because other wedge tests using adherends treated in 10-ppm NTMP solutions gave results similar to those in Fig. 7 (see below), the performance illustrated in Fig. 7 is considered typical of the 10-ppm NTMP solution treatment.

We also performed wedge tests on adherends treated with NTMP at 80°C, where the surface coverage was ~ 2 to 3 times higher than that on adherends treated at room temperature (Table I). The results (Fig. 9) demonstrate that no improvement in bond durability is achieved by increasing the NTMP coverage above the saturation coverage achieved with room temperature treatments.

Wedge tests performed using NTMP, HMP, and AMP demonstrate (Fig. 10) that all of these inhibitors improve bond durability, with the NTMP treatment effecting the most significant improvement. The inhibitor concentrations used for these treatments were chosen so that the solution normality was the same in each case; that is, the concentrations were chosen so that the solution contained the same number of molecules per volume of solution. Thus, a 33-ppm solution (by weight) of HMP or AMP is equivalent to a 100-ppm NTMP solution since the solutions contain the same number of molecules for adsorption on active surface sites.

Finally, wedge tests using phosphoric acid as the inhibitor (Fig. 11) showed little or no improvement in bond durability compared with the untreated FPL adherend. In fact, intermediate and low concentrations of PA appear to somewhat degrade the performance of FPL adherends. This result is surprising because we expected improvements in bond durability from using PA, based on the increase in incubation time of PA-treated coupons. Possible reasons for this are discussed below.

D. XPS Measurements of Failed Surfaces from Wedge Tests

To define the locus of failure more precisely, we broke apart selected wedge test samples, exposing the fracture surface, and analyzed the matching surfaces using XPS. The results of this analysis (Table III) reveal several significant factors that are important for understanding the wedge test results. First, the matching FPL adherend surfaces exhibited nearly identical surface composition, with substantial amounts of Al seen on both sides of the fracture. In the case of the FPL adherend

treated in NTMP at room temperature, the matching surfaces differed somewhat in composition with somewhat less Al and somewhat more C seen on the adhesive side of the failure than on the Al side. Substantial amounts of Al were still observed on the adhesive however.

The results for the FPL adherend treated in NTMP at 80°C exhibited a marked difference in surface chemistry between the Al and adhesive failure surfaces. Although the Al fracture surface was similar in composition to that of untreated FPL adherends (with the exception of the small amount of P), the adhesive exhibited substantially less Al and more C than was seen on the untreated surfaces. A small amount of P was also observed on this surface. The FPL adherends treated with 3.3- and 33-ppm PA were similar to the untreated FPL adherend, and the sample treated with 66-ppm PA was similar to the FPL adherend treated in NTMP at 80°C.

IV. DISCUSSION

The wedge test results described here clearly demonstrate that bond durability of FPL-etched adherends can be significantly improved using hydration inhibitors. Moreover, the durability of FPL-etched adherends treated with NTMP approaches that of PAA adherends. The control of bond durability through adherend surface chemistry further suggests that the conversion of Al-oxide to hydroxide is a significant factor in determining the performance of adhesive bonds in moist environments. Several results require additional discussion however.

Consider first the results for surface coverage as a function of solution concentration (Fig. 6). The NTMP coverage saturates between 0.15 and 0.20 above a solution concentration of about 5 ppm, suggesting that monolayer coverage is achieved in this case. The coverage of AMP and HMP also appears to saturate, but at lower values (0.05 to 0.06). If we assume that the saturation coverages of NTMP, AMP, and HMP are indeed monolayer and that in each case the adsorbed molecules are attached to the same number of active sites on the Al-oxide surface, then the coverage values can be explained by assuming that only one leg of the NTMP molecule actually attaches to the Al-oxide surfaces, the other two legs remain unreacted (Fig. 12). This then means that for AMP and HMP there should be one P atom per two active sites, whereas for NTMP, there should be three P atoms per two active sites, and the coverage should be in the ratio of 1 to 3 as observed by XPS.

Using these same arguments for the PA case, we found that the observed coverage ($\sim$ 0.1) is too large to account for full coverage

of active sites, assuming one P atom per three active sites, and it must be assumed that the density of adsorbed molecules is larger than the number of active sites, presumably because the PA coverage of 0.1 represents multilayers of phosphate molecules and not simply a monolayer. In the same way, the coverage produced by the 80°C NTMP treatment is probably several NTMP layers thick.

The reason these coverage values and adsorption models are important will become clear in the following discussion of wedge test results.

Consider now the wedge test results shown in Figs. 8 and 9 for NTMP-treated FPL adherends. The decrease in maximum crack extension with increasing NTMP concentration suggests that saturation coverage of the room-temperature treatment (P/Al ratio ~ 0.15) is required to realize maximum improvements in bond durability. The absence of any further decrease in maximum crack extension with adherends that were treated at 80°C and had coverages 2 to 3 times larger than the saturation values observed at room temperature, suggests further that the saturation coverage is sufficient to achieve maximum benefit from the NTMP treatment. Indeed, the wedge tests (Fig. 9) indicate that coverages larger than the saturation value result in a small degradation of bond durability.

Wedge tests using NTMP, HMP, and AMP (Fig. 10) demonstrate that, with constant-normality treatment solutions, NTMP-treated adherends exhibit a smaller crack extension at long exposures compared with either HMP or AMP. Moreover, the arguments given above suggest that all of these inhibitors are present as monolayer films on the adherend surface. Thus, because NTMP appears to perform better than HMP or AMP, the mechanism

whereby bond durability is improved must involve either a) the effectiveness of the particular inhibitor in preventing the conversion of Al-oxide to hydroxide, b) chemical interaction of the adsorbed inhibitor molecules and adhesive molecules, or c) both. Limited data on incubation time (Table II) suggest that NTMP is somewhat more effective than AMP in inhibiting the hydration reaction, so that this may be partially responsible for the apparent better performance of NTMP-treated adherends.

Coupling of NTMP and adhesive molecules may also be important, however. Consider, for example, the wedge test results for PA-treated adherends (Fig. 11), which showed no decrease in crack extension compared with untreated adherends, despite the effectiveness of PA treatments in inhibiting the oxide-to-hydroxide conversion (Table II). The XPS results from fracture surfaces (Table III) suggest that, in the case of the 66-ppm PA treatment, the crack propagated at the PA film/adhesive interface since little Al was found on the adhesive side of the failure, and a small amount of P was detected on the Al side. Even though PA inhibits the hydration reaction, the PA/adhesive bonds are not resistant to attack by moisture and, therefore, provide an easy crack propagation path; PA is not effective in improving the durability of FPL adherends. In the samples treated with 3.3- and 33-ppm PA, the inhibiting effect of PA is apparently not adequate for preventing the oxide-to-hydroxide reaction and degradation of the bond durability by moisture.

In support of these arguments, consider the XPS results of failed wedge-test panels treated with NTMP at 80°C (Table III). These suggest that the crack propagated between the NTMP/adhesive interface or through

the NTMP layer itself (since P is observed on both sides of the failure). However, in this case, the bond durability was improved substantially over that in untreated adherends (Fig. 9). Recall that the coverage data suggested that the PA and 80°C NTMP treatments produce multilayer surface films. Thus, the apparent common locus of failure, but markedly different wedge test performance, in these two cases implies that the PA-adhesive bond is not resistant to moisture attack, whereas the NTMP-adhesive bond is.

What then accounts for the excellent performance of PAA adherends, since the coverage of PAA- and PA-treated FPL adherends is the same and the adherends might be expected to behave in a similar fashion? There is a substantial difference in the oxide morphology produced by the FPL and PAA processes (Figs. 1 and 2). Oxides produced by the PAA process interlock with the adhesive through a substantially thicker oxide layer than those produced by FPL. Physical interlocking in the PAA case should be more efficient, and the bond performance even less dependent on chemical reactions of oxide and adhesive than adherends prepared using FPL. The presumed degradation of chemical bonding between the PA film and adhesive should have little affect on the bond durability of PAA adherends because the subetantial physical interlocking of oxide and adhesive prevents crack propagation. The inhibiting nature of the PA film stabilizes the PAA oxide structure against attack by moisture, resulting in excellent bond durability. The FPL adherends exhibit a degree of surface roughness that is apparently not sufficient to prevent crack propagation between a multilayer PA film and the adhesive. Bond durability in this case is,

therefore, not improved by PA treatments over that obtained in untreated FPL adherends.

The use of NTMP on FPL adherends does produce a marked improvement in bond durability over untreated adherends independent of the presumed monolayer or multilayer coverage. This suggests that the NTMP film, in addition to inhibiting the hydration reaction, also reacts with the adhesive. This might be understood by examining the structure of the NTMP molecule (Fig. 4) and the possible adsorption model (Fig. 12). One phosphonic acid group attaches to the Al-oxide surface, and the other two are unreacted. These can then react with the epoxy adhesive to form strong, moisture-resistant bonds. Thus, we suggest that NTMP serves to prevent oxide-to-hydroxide conversion and, at the same time, to produce good chemical bonding between the adherend and adhesive.

In summary, hydration inhibitors can be used to improve the bond durability of adherends etched in FPL. Use of NTMP improves the durability of FPL-prepared 2024Al adherends to the point where they behave in nearly the same manner as adherends prepared with the PAA process. Analysis of the results suggest that an inhibitor's effectiveness depends on both its ability to inhibit the conversion of Al-oxide to hydroxide and to form chemical bonds with the adhesive.

V. REFERENCES

1. J.D. Venables, D.K. McNamara, J.M. Chen, T.S. Sun, and R.L. Hopping: "Oxide Morphologies on Aluminum Prepared for Adhesive Bonding," Applications of Surface Science (1979) Vol. 3, pp. 88-98.

2. J.D. Venables, D.K. McNamara, J.M. Chen, B.M. Ditchek, T.I. Morgenthaler, and T.S. Sun: "Effect of Moisture on Adhesively Bonded Aluminum Structures," Proc. 12th National SAMPE Tech. Conf. (1980), Seattle, Washington.

3. G.S. Kabayashi and D.J. Donnelly: Boeing Co. Report No. DG 41517 (February 1974).

4. G.D. Davis, T.S. Sun, J.S. Ahearn, and J.D. Venables: "Application of Surface Behavior Diagrams to the Study of Hydration of Phosphoric Acid Anodized Aluminum," submitted to J. Mater. Sci.

Table I

Inhibitor Surface Coverage at Saturation as Determined by XPS for 2024Al Adherends Prepared by the FPL Process

Inibitor and Treatment Temperature	Surface Coverage (P/Al ratio)
NTMP, RT	0.15
NTMP, 80°C	0.40
AMP, RT	0.05
HMP, RT	0.05
PA, RT	0.10

Table II

Incubation Time for FPL-Etched 2024Al

Surfaces Treated in Different Hydration Inhibitors

Sample Description	Incubation Time (min)
FPL no treatment	1.5-2.0†
FPL + 10-ppm NTMP	360†
FPL + 100-ppm NTMP	indefinite†
FPL + 100-ppm NTMP	12†
FPL + 10-ppm AMP	5.5†
FPL + 10-ppm NTMP	37*
FPL + 10-ppm PA	18*

† Determined by visual observation
* Determined by ellipsometry, comparison tests

Table III

Surface Composition of Failed Surfaces as Determined by XPS

Sample Description	Element (at %)							
	Al		O		P		C	
	A*	B*	A*	B*	A*	B*	A*	B*
FPL	16	18	52	45	-	-	32	37
FPL + 10-ppm NTMP, RT	19	11	51	38	-	-	30	51
FPL + 10-ppm NTMP, 80°C	14	2.5	40	25	1	0.5	45	72
FPL + 3.3-ppm PA	18	15	46	43	-	-	36	42
FPL + 33-ppm PA	27	17	52	42	-	-	21	41
FPL + 66-ppm PA	25	2	49	25	0.6	-	25	73

* A is Al side of failure and B is matching adhesive side of failure.

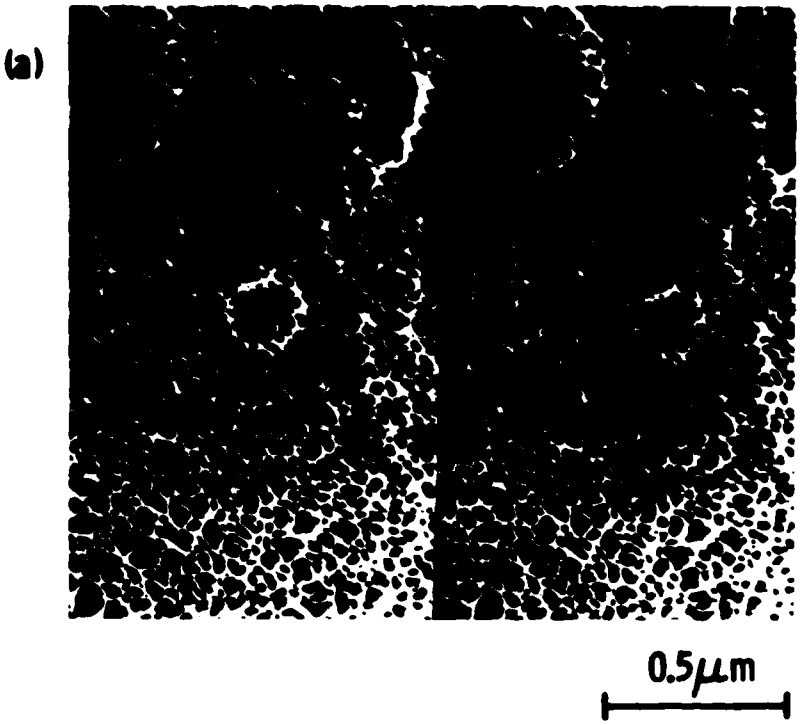

Figure 1. Stereo micrograph of Al oxide morphology on FPL adherends and schematic of oxide structure (1).

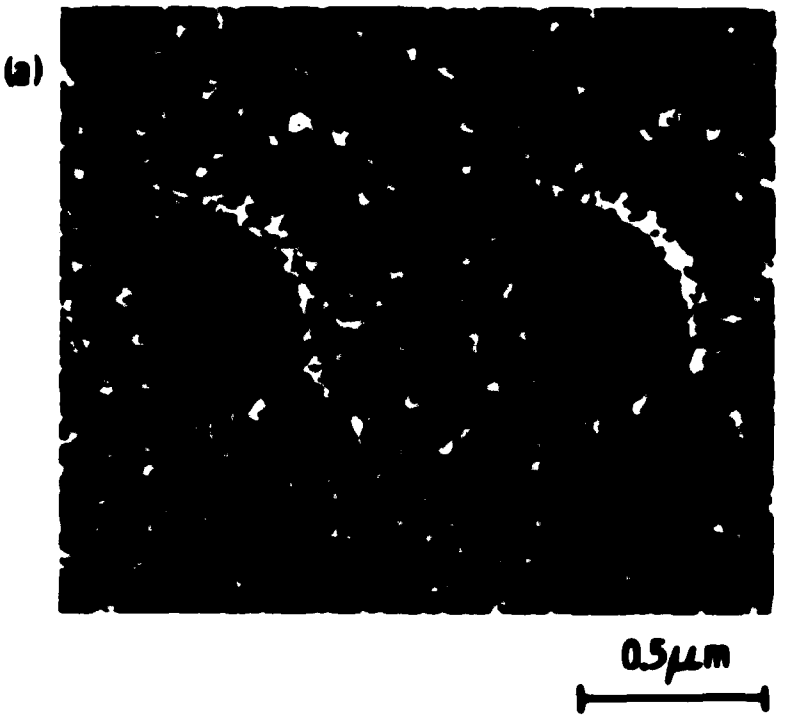

Figure 2. Stereo micrograph of Al oxide morphology on PAA adherends and schematic of oxide structure (1).

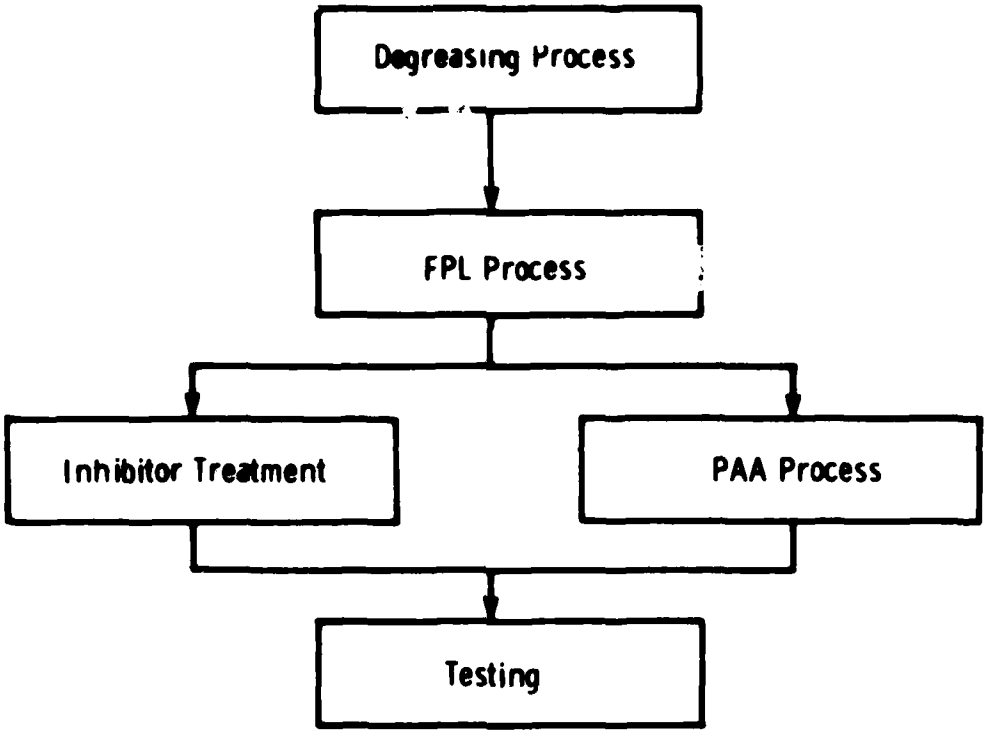

Figure 3. Flow chart for preparation of 2024Al surfaces.

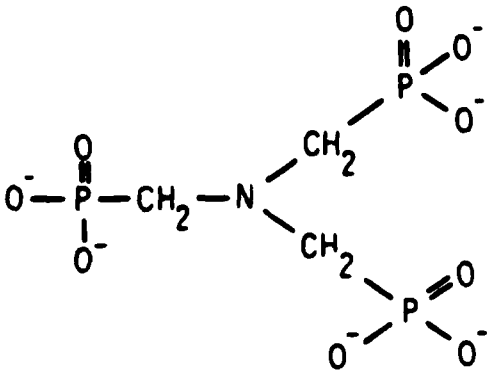

Nitrilotris
(Methylene) Phosphonic Acid

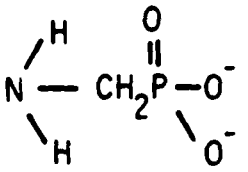

Amino Methyl Phosphonic Acid

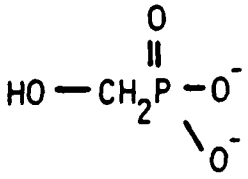

Hydroxy Methyl Phosphonic Acid

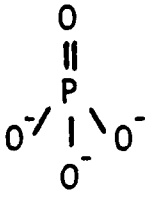

Phosphoric Acid

Figure 4. Schematic of deprotonated inhibitor molecules.

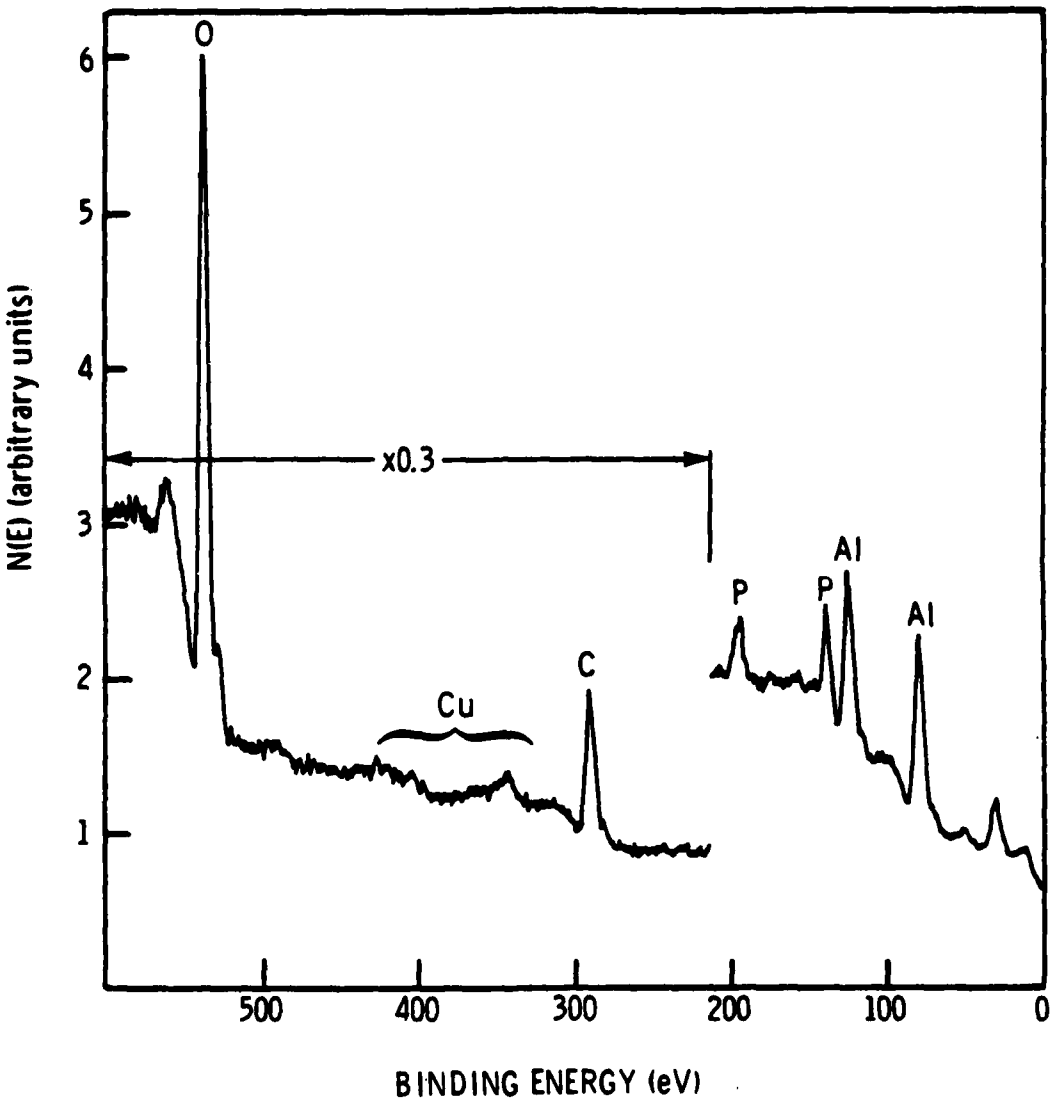

Figure 5. XPS spectra of NTMP-treated 2024Al surface previously etched in FPL. The room-temperature NTMP solution concentration was 10 ppm.

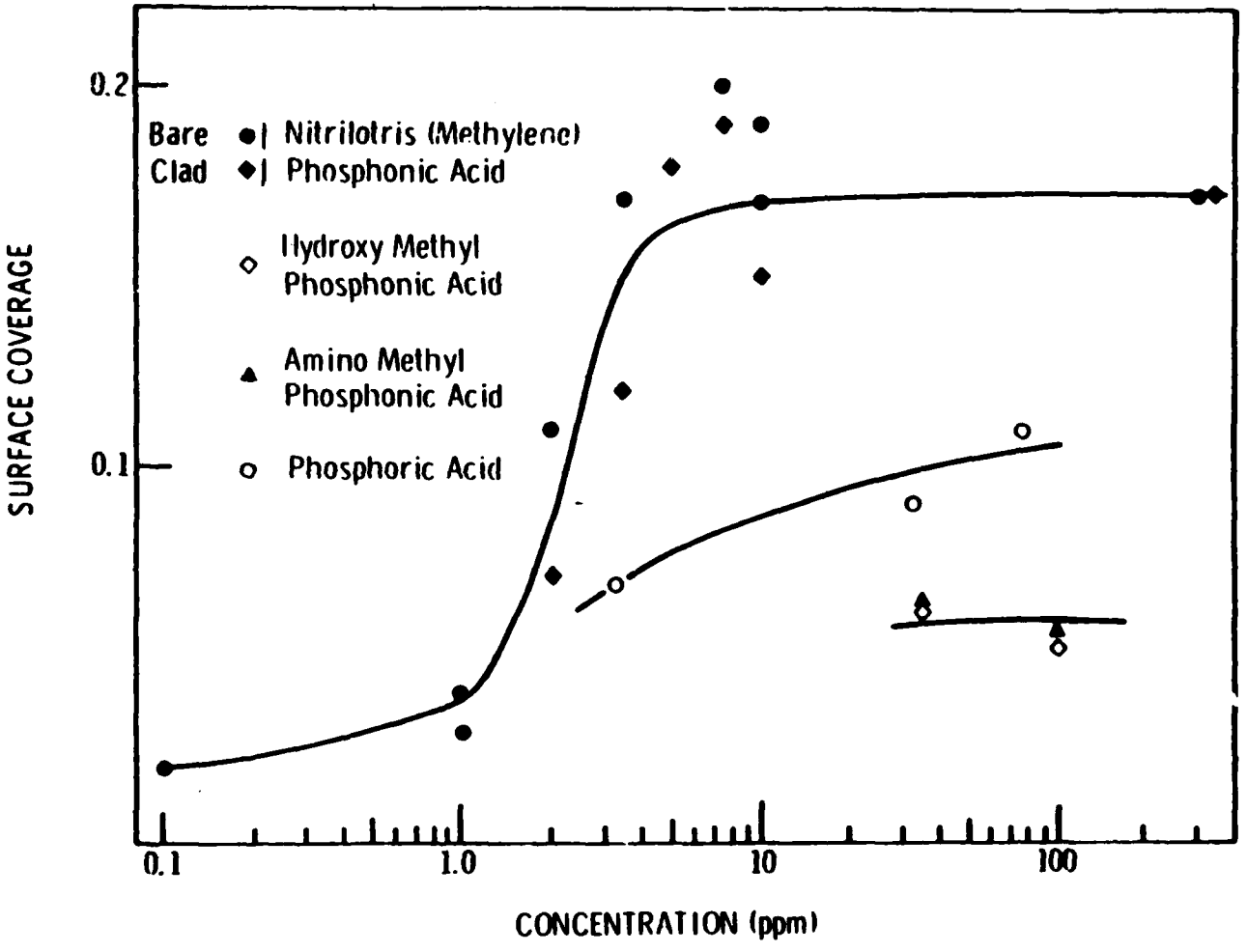

Figure 6. Inhibitor surface coverage (P/Al ratio as determined by XPS) of FPL-etched 2024Al as a function of inhibitor solution concentration.

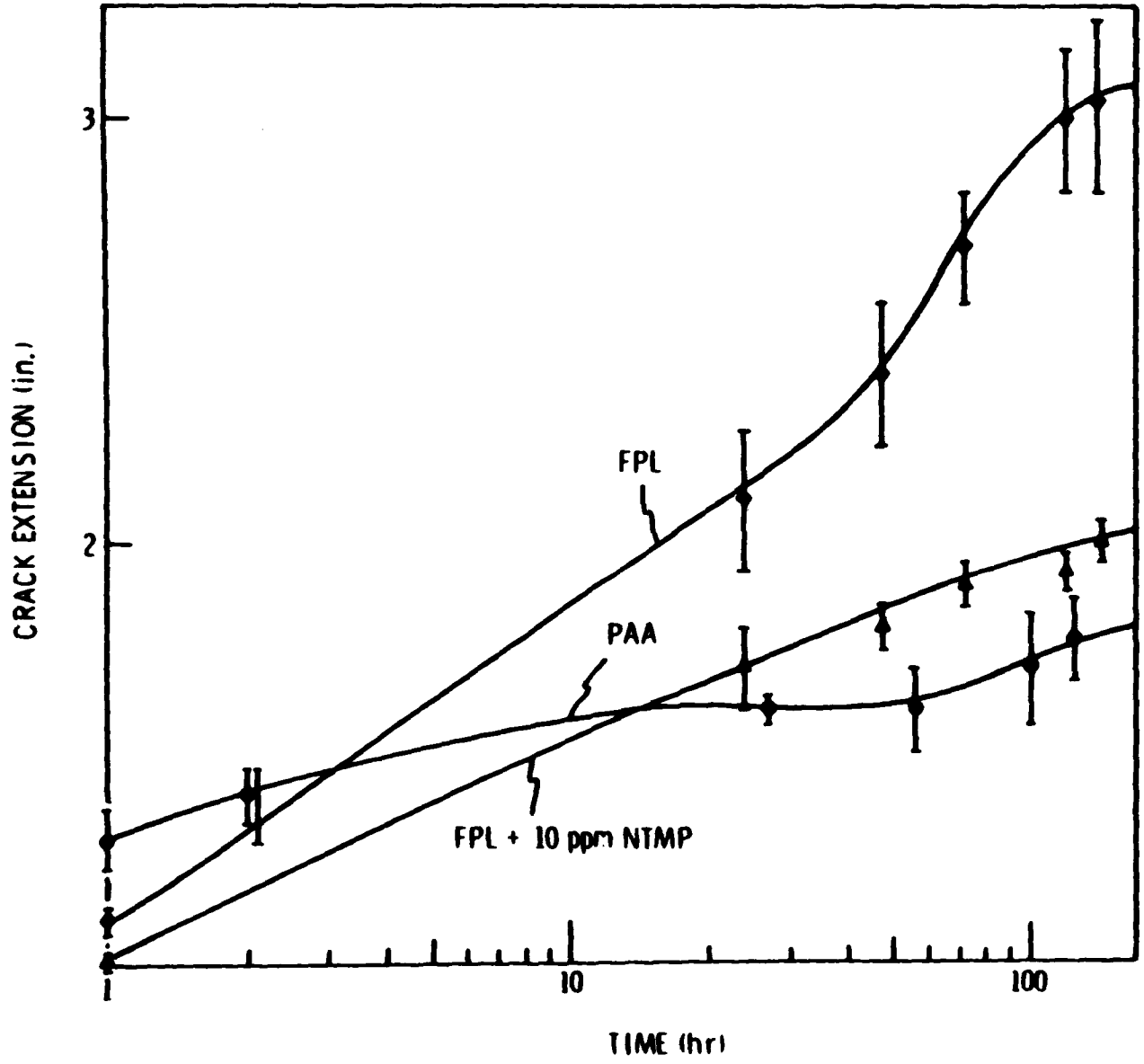

Figure 7. Crack extension vs time for FPL and PAA adherends and for FPL adherends treated with a 10-ppm NTMP solution.

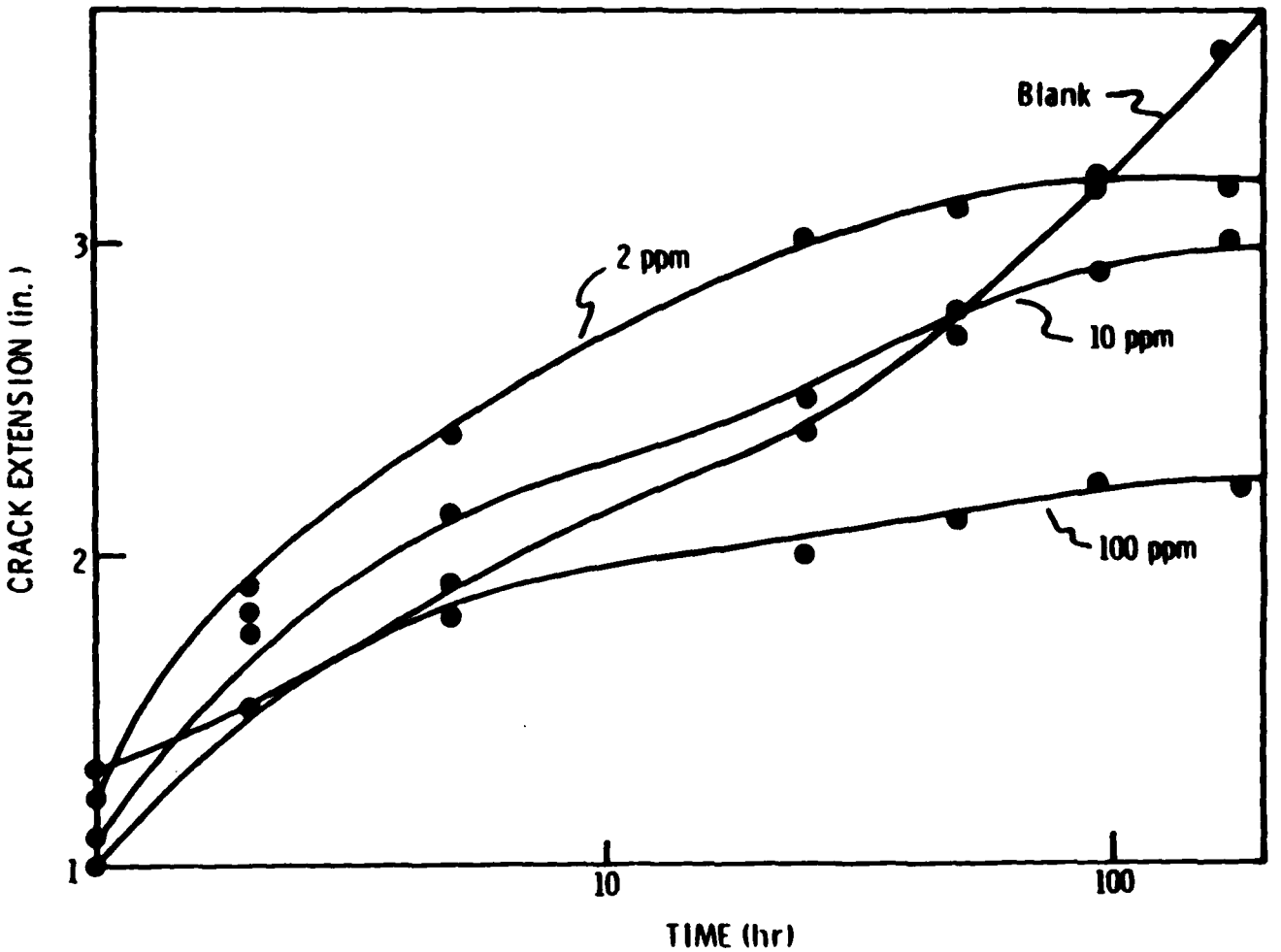

Figure 8. Crack extension vs time for FPL adherends treated with 2-, 10-, and 100-ppm NTMP solutions.

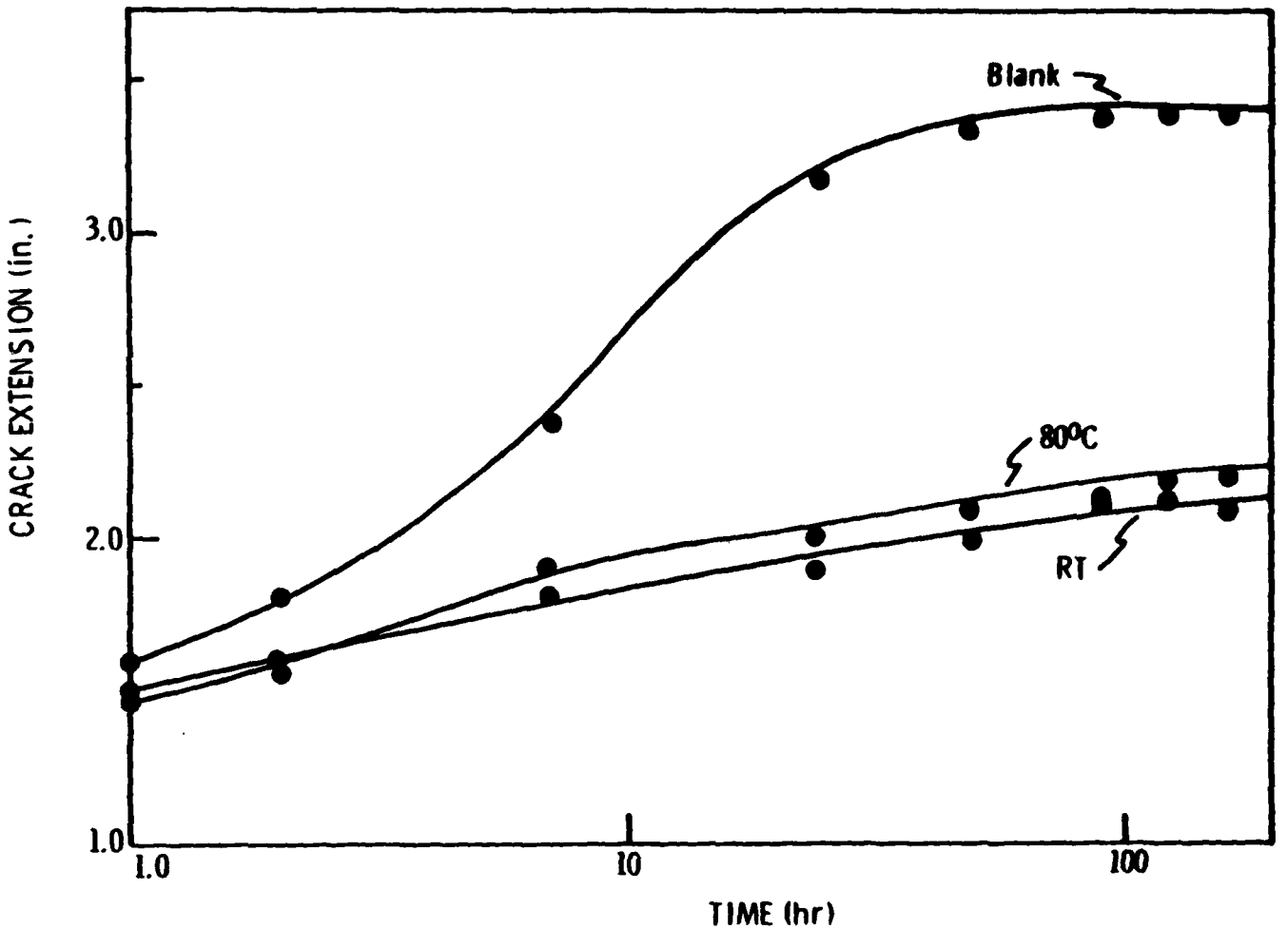

Figure 9. Crack extension vs time for FPL adherends treated with a 10-ppm NTMP solution at room temperature and 80°C.

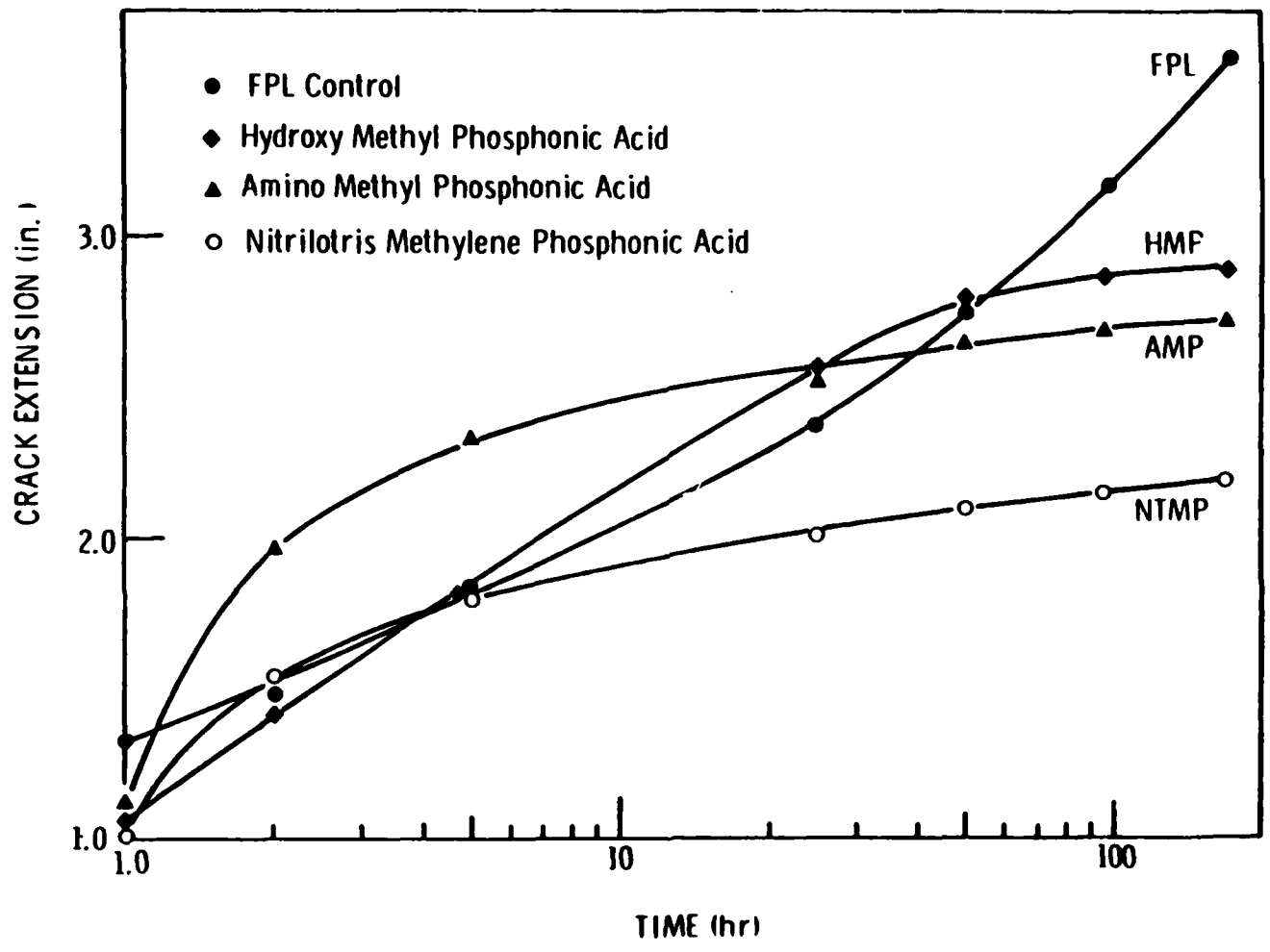

Figure 10. Crack extension vs time for FPL adherends treated with 100-ppm NTMP solution or a 33-ppm AMP or HMP solution.

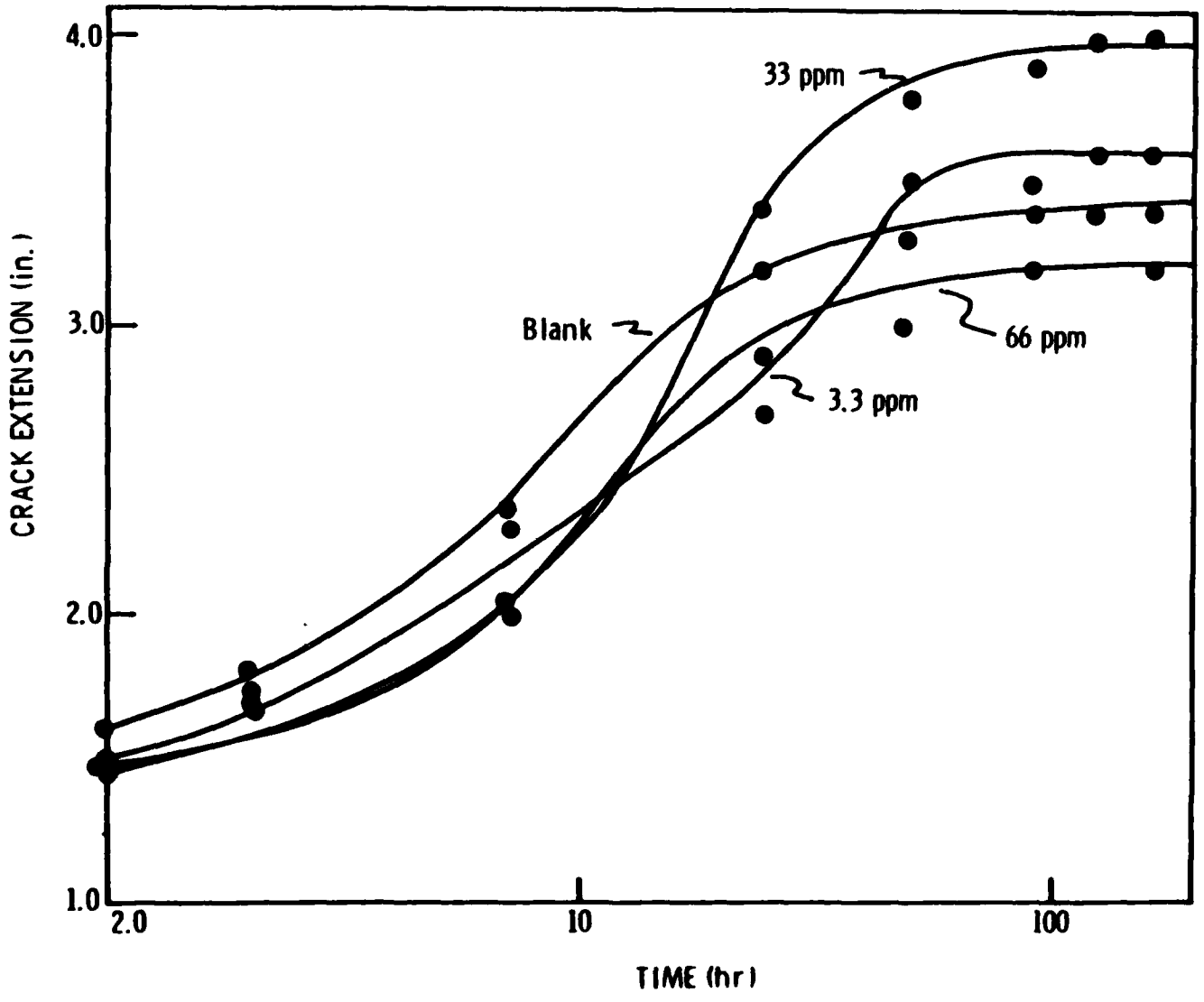

Figure 11. Crack extension vs time for FPL adherends treated with 3.3-, 33-, or 66-ppm PA solutions.

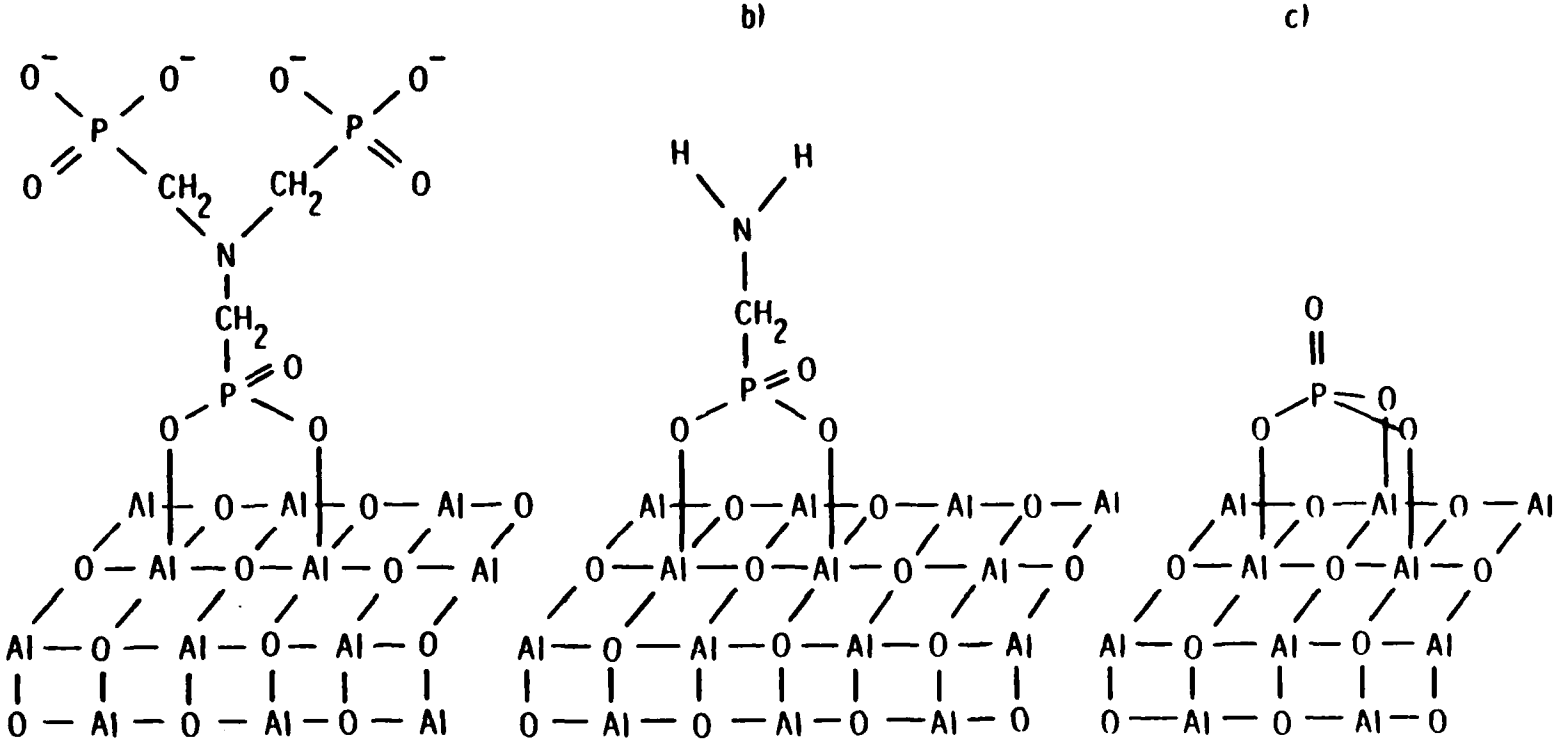

Figure 12. Models of adsorption of hydration inhibitors. a) NTMP, b) AMP, and c) PA.


DATE
ILME